frontiers | Frontiers in Materials

TYPE Original Research
PUBLISHED 02 December 2022
DOI 10.3389/fmats.2022.1056600

OPEN ACCESS

EDITED BY
Ruirui Qiao,
Australian Institute for Bioengineering and Nanotechnology, University of Queensland, Australia

REVIEWED BY
Zhaoting Li,
University of Wisconsin-Madison, United States
Honglin Jin,
Huazhong Agricultural University, China
Hao Song,
Australian Institute for Bioengineering and Nanotechnology, University of Queensland, Australia

*CORRESPONDENCE
Hong Ge,
gehong616@126.com
Yingqiu Qi,
qiyq@zzu.edu.cn

SPECIALTY SECTION
This article was submitted to Smart Materials, a section of the journal Frontiers in Materials

RECEIVED 29 September 2022
ACCEPTED 21 November 2022
PUBLISHED 02 December 2022

CITATION
Huang T, Sun X, Meng X, Chen M, Li Y, Du S, Qi Y and Ge H (2022), Peptide self-assembled nanomedicine induces antitumor immunity by blocking the PD-1/PD-L1 axis.
Front. Mater. 9:1056600.
doi: 10.3389/fmats.2022.1056600

Peptide self-assembled nanomedicine induces antitumor immunity by blocking the PD-1/PD-L1 axis

Tao Huang[1], Xianfu Sun[1], Xiaocao Meng[2], Mengdie Chen[2], Yapeng Li[2], Shengnan Du[2], Yingqiu Qi[2]* and Hong Ge[3]*

[1]Department of Breast Disease, Henan Breast Cancer Center, The Affiliated Cancer Hospital of Zhengzhou University and Henan Cancer Hospital, Zhengzhou, China, [2]Department of Pharmacology, School of Basic Medical Sciences, Zhengzhou University, Zhengzhou, Henan, China, [3]Department of Radiation Oncology, The Affiliated Cancer Hospital of Zhengzhou University and Henan Cancer Hospital, Zhengzhou, China

The development of immune checkpoint inhibitors (ICIs) revolutionizes cancer treatment, which has been applied in the treatment of several kinds of malignancies in the clinic. Due to their specific affinity and controllable cost, the emerging peptide-based ICI therapeutics have attracted great attention. However, peptide-based drugs generally show poor bioavailability and a short *in vivo* half-life. Peptide-based nanomedicine is a promising approach to increase the efficacy of therapeutic peptides. In this work, an amphiphilic peptide based on the reported D-peptide for ICIs has been developed. The constructed amphiphilic peptide can self-assemble into a stable nanostructure (noted as CD-NPs). The prepared CD-NPs have a spherical shape with a hydrodynamic size of about 35 nm. *In vivo* studies show that the prepared nanomedicine can effectively inhibit tumor growth in 4T1 tumor-bearing mice. Moreover, we found that the CD-NPs increase the infiltration of effector T cells and natural killer cells as well as the immune cytokines in the tumor tissues, implying that they activated the immune response for antitumor activity. Finally, no obvious changes in the major organs, tissues, or the body weight caused by the nanomedicine can be observed, demonstrating their good biocompatibility. Taken together, this study provides a basic idea for designing a novel peptide-based nanomedicine for enhanced antitumor efficacy by enhancing the blockade of ICIs and activating the immune response.

KEYWORDS

immune checkpoint inhibitors (ICIs), nanomedicine, antitumor immunity, peptides, PD-L1, PD-1

Introduction

Checkpoint blockade-based immunotherapy that evokes the host immunity to fight against cancers has resulted in unprecedented rates of effective responses in increasing kinds of malignancies (such as colon cancer and breast cancer) (Marin-Acevedo et al., 2018; Robert, 2020; Singh et al., 2020). Immune checkpoint inhibitors (ICIs) mainly suppressed the activity of negative regulatory molecules of immunity (such as cytotoxic T-lymphocyte-associated protein 4) or blocked the interactions between the checkpoint molecules (e.g., programmed cell death 1 (PD-1) or programmed cell death 1 ligand 1 (PD-L1)) and their corresponding ligands (Mahoney et al., 2015; Meng et al., 2015; Rezvani et al., 2017; Gong et al., 2021; Hu et al., 2021). Upon the checkpoint being blocked, the immune recognition and cancer surveillance of host immunity will be restored (Chen and Mellman, 2013; Dempke et al., 2017; Darvin et al., 2018). Among these ICI-based therapeutic drugs, PD-1 or PD-L1 antibodies have the most outstanding clinical treatment achievements (Acurcio et al., 2018; Li et al., 2020; Li et al., 2022). Despite encouraging clinical efficacy, the non-negligible safety risk caused by immune-related adverse events and high costs limited the population of patients who benefited from these therapeutics.

By virtue of the flexibility of sequence design, controllable preparation cost, and high affinity to specific biomarkers, peptides have plenteous application potential in mimicking antibodies in the clinic (Cui et al., 2010; Gautam et al., 2014; Delfi et al., 2021; Gong et al., 2021). Numerous efforts have been devoted to developing ICI-based peptides. With the effective phase display technology, Gao and coworkers screened a ^{D}PPA-1 peptide, which can competitively bind to PD-L1 and consequently block the PD-1/PD-L1 axis to restore the recognition and killing ability of immunity to cancer cells (Blank and Mackensen, 2007; Chang et al., 2015; Sun et al., 2018). However, facing the challenge in the pharmacokinetics of free peptides, such as short half-life time and vulnerability to serum peptidase *in vivo*, the developed ^{D}PPA-1 must be administered intratumorally, which limited its translational potential in the clinic.

Considering the weakness of free therapeutic peptides, chemical modifying of the hydrophilic peptide to be amphiphilic and consequently self-assembling into stable nanomicelles under physiological conditions are a practicable strategy (Zhao et al., 2014; Cheng et al., 2018; Du et al., 2018; Yu et al., 2021). By virtue of the advantage of nanosize, the self-assembled nanomicelles can accumulate in the tumor tissue by enhanced permeability and retention effect (Eskandari et al., 2017; Robert, 2020; Taleb et al., 2021). In this work, ^{D}PPA-1 was covalently

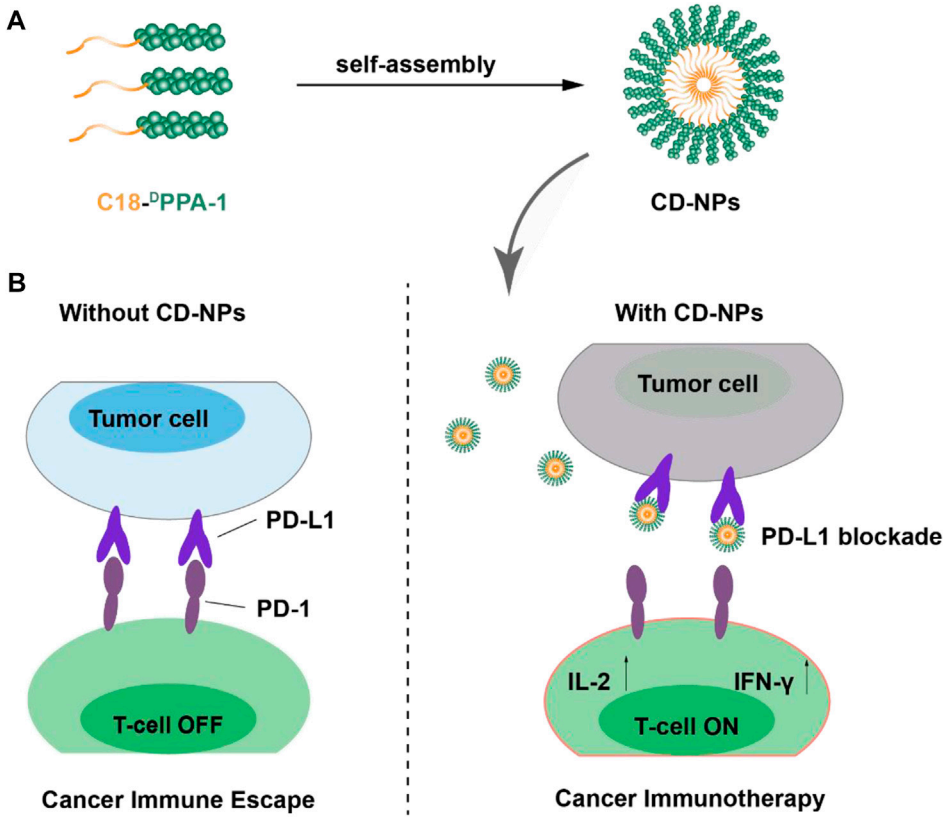

SCHEME 1
Schematic illustration of the preparation of CD-NPs and the antitumor mechanism of CD-NP-mediated cancer immunotherapy.

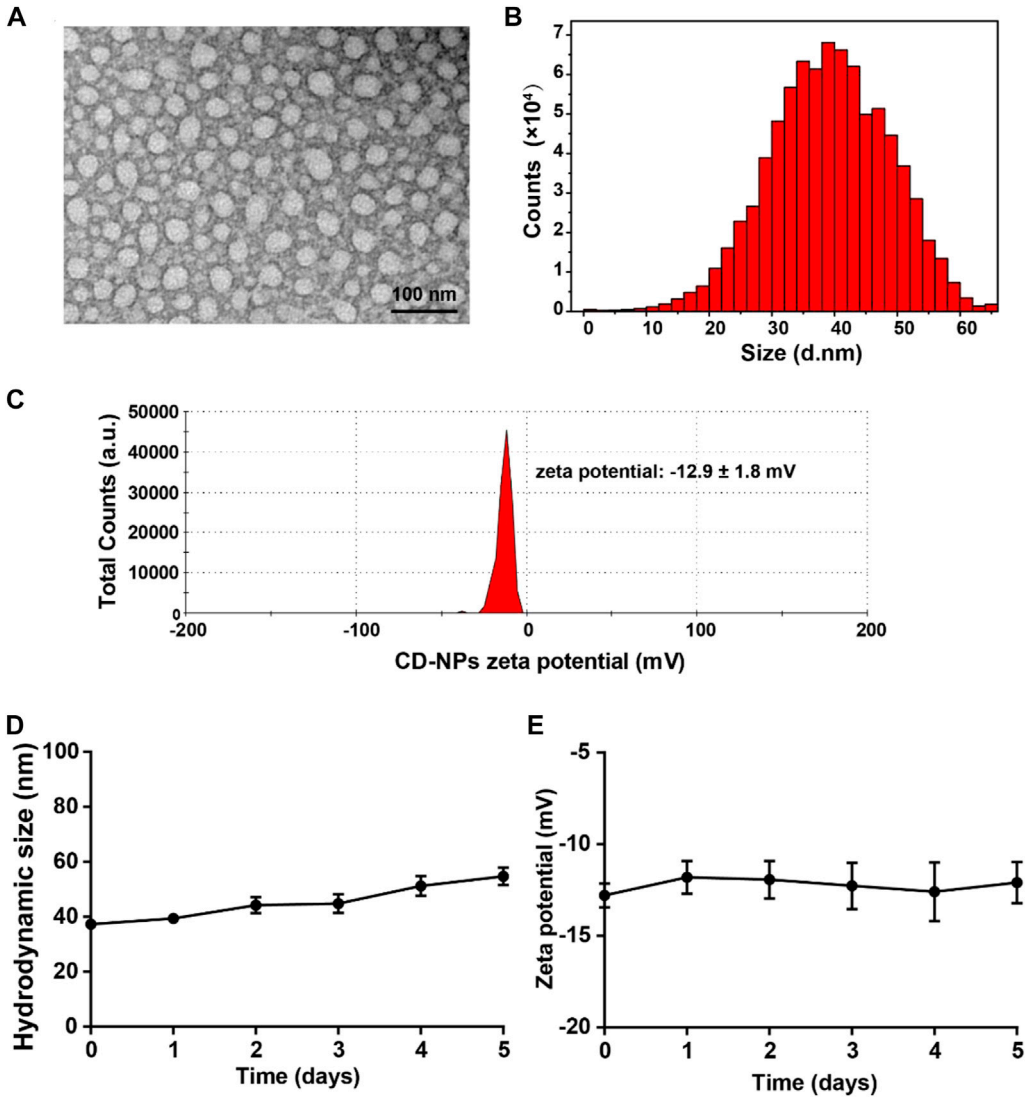

FIGURE 1
Characterization of the peptide self-assembled nanomedicine. **(A)** TEM images of prepared CD-NPs. **(B)** Hydrodynamic size distribution and **(C)** zeta potential of CD-NPs in PBS measured by DLS. **(D)** Changes in hydrodynamic size and **(E)** zeta potential of CD-NPs incubated in PBS for 5 days.

modified with hydrophobic octadecanoic acid, and an amphiphilic peptide C18-^{D}PPA-1 was obtained. As shown in Scheme 1A, the prepared C18-^{D}PPA-1 can self-assemble into a stable spherical nanomicelle (noted as CD-NPs) with a hydrodynamic size of about 35 nm. After intravenously administered into 4T1 tumor-bearing mice, the CD-NPs can effectively suppress the growth of the tumor. Further research revealed that the CD-NPs can activate the host immunity of mice, including improving the infiltration of T lymphocytes (T cells) and natural killer (NK) cells in tumor tissues, along with increasing the level of antitumor immune cytokines, such as interferon-γ (IFN-γ) and interleukin 2 (IL-2) Scheme 1B. In addition, there is no obvious body weight loss in mice during the treatment period, and negligible changes in serum biochemical analysis and histopathological analysis of major organs can be observed. Taken together, this work developed a practical peptide-based nanomedicine for ICIs, which has an effective antitumor ability, as well as satisfying biocompatibility.

Materials and methods

Materials and reagents

Sterile PBS, RPMI-1640 cell culture media, and tissue-fixing buffer were purchased from Servicebio (Wuhan, China). The ^{D}PPA-1 and C18-^{D}PPA-1 peptides were purchased from Anhui Guoping Pharmaceutical Co., Ltd. (Hefei, China). Trypsin and pentobarbital sodium were purchased from

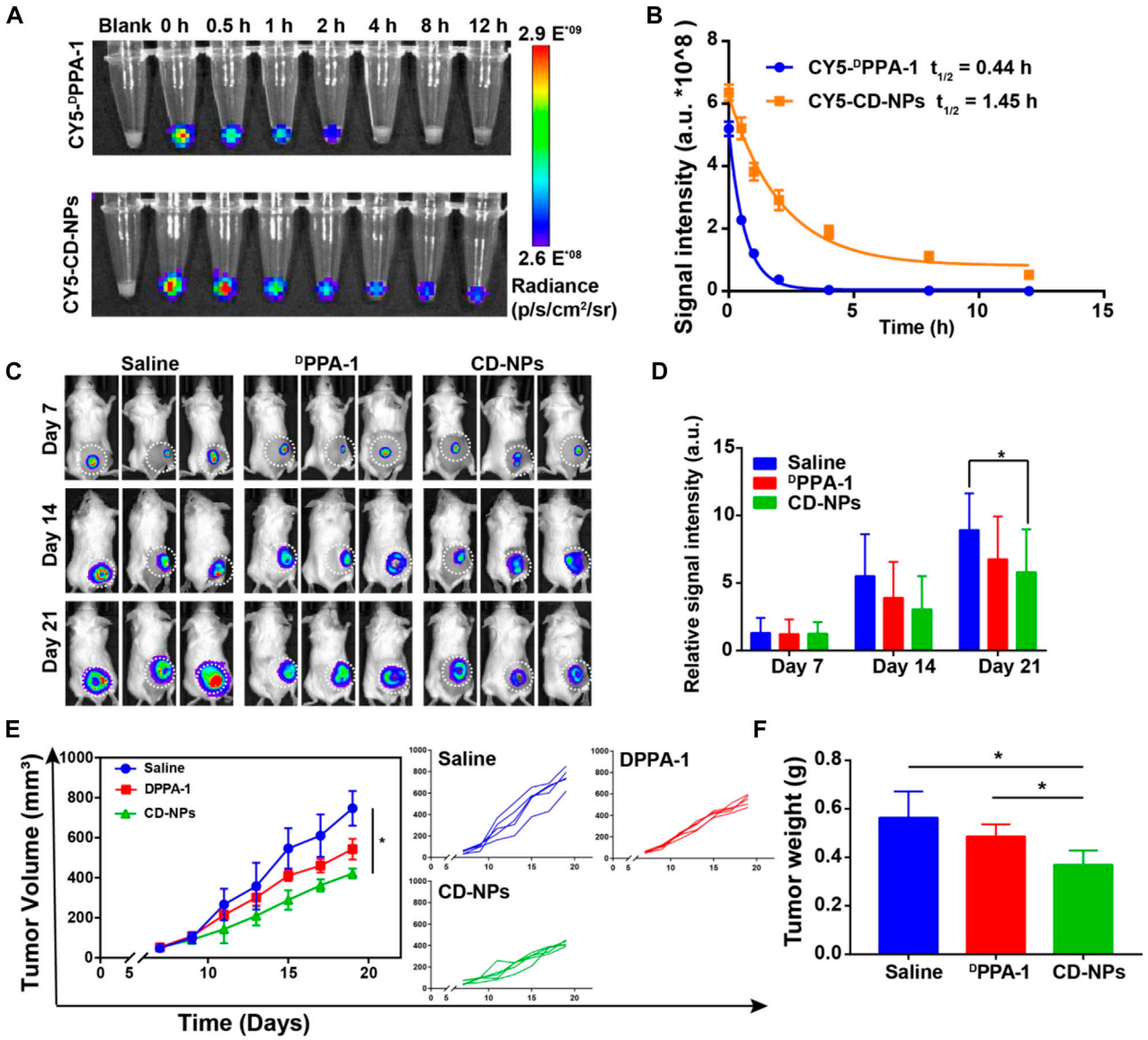

FIGURE 2
Pharmacokinetics and antitumor effects of CD-NPs *in vivo*. **(A)** Fluorescence images and **(B)** semi-quantitative analysis of blood collected at indicated time points from 4T1-luci tumor-bearing mice injected with CY5-labeled DPPA-1 or CD-NPs ($n = 3$). **(C)** Bioluminescence images and **(D)** corresponding semi-quantitative analysis of 4T1-luci tumor-bearing mice at indicated time points after treatment with different formulations ($n = 3$). **(E)** Growth curves of tumors from mice treated with various formulations. **(F)** Tumor weights of mice treated with various formulations ($n = 5$). *$p < 0.05$.

Solarbio Science & Technology Co., Ltd. (Beijing, China). The matrix gel was purchased from Corning (United States). Heparin sodium was purchased from Yuanye Bio-Technology Co., Ltd. (Shanghai). The fixation buffer, perm/wash, PE anti-mouse CD8α antibody, FITC anti-mouse CD3 antibody, PE/Cyanine7 anti-mouse IFN-γ antibody, Alexa Fluor® 488 anti-mouse CD49b antibody, and Alexa Fluor® 647 anti-mouse CD69 antibody were purchased from BioLegend (United States), and fetal bovine serum was purchased from Biological Industries. IFN-γ and IL-2 ELISA kits were purchased from Pengpai Bio-Technology Co., Ltd. (Shanghai).

Equipment

A 0–150 mm caliper (DeguoMNT), 5810R ultra-speed centrifuge (Eppendorf, German), DV215CD digital balance

(OHAUS, United States), IVIS (PerkinElmer, United States), inverse microscope (Olympus, Japan), and digital sonicator (Jiekang, Dongguan) were used for this experiment.

Animals

BALB/c mice weighing 18–22 g (female, 6–8 weeks old) were purchased from the Animal Center of Zhengzhou University (Henan, China).

Preparation of self-assembled peptide nanomedicine

A measure of 1 mg of C18-^{D}PPA-1 peptide was dissolved in 10 μL DMSO. Subsequently, the peptide was slowly distributed into 1 ml of PBS using a 1-ml syringe, followed by sonication for 15 min. Then, the mixture was placed at room temperature for 1–2 h to form peptide self-assembled nanomedicine.

Characterization of the peptide self-assembled nanomedicine

The morphology of the peptide self-assembled nanomedicine was characterized by transmission electron microscopy (TEM) as follows: briefly, 10 μL of the nanomedicine was dropped on the carbon-supported copper grid and allowed to sit for 10–15 min for air-drying. Then, 7 μl of uranyl acetate dihydrate was added onto the sample for staining purpose. After 3 min, the extra uranyl acetate dihydrate was absorbed gently using a piece of filter paper. When the dye dried, the sample on the copper grid was placed into the sample chamber of TEM for morphological study.

Antitumor efficiency study

To investigate the antitumor efficiency by the nanomedicine *in vivo*, the 4T1 tumor-bearing mouse model was constructed. When the tumor volume reached about 200 mm^3, mice were separated into three groups randomly (n = 5), which were treated with PBS, ^{D}PPA-1 peptide, or CD-NPs every other day within 2 weeks. Before each injection of nanomedicine or controls, the body weights of mice and the lengths (L) and widths (W) of tumors were measured and recorded. The tumor volume was calculated using the equation: $(L \times W^2)/2$. In addition, luciferase substrate was intraperitoneally injected at days 7, 14, and 21 after tumor planting to monitor the tumor volume *via* the IVIS imaging system. After therapy, mice were euthanized for tumor weight and volume measurement.

Study of the population of T cells and NK cells in the tumor

After the treatment, mice were sacrificed. Tumors were harvested, and a small section of tumor in each group was lysed with tissue lysis buffer containing collagenase, hyaluronidase, and 1% trypsin at 37°C for 30 min, followed by termination of lysis with cell culture media containing 2% FBS to obtain the cell mixture, which was filtered through 70-μm mesh sieves for single-cell suspension. The single-cell suspension was stored for the analysis of immune cell populations. Briefly, a part of the single-cell suspension was incubated with anti-CD3-FITC and anti-CD8α antibodies on ice in the dark for 40 min. Then, the cells were washed twice with FBS-free media and permeabilized with 500 μL perm/wash buffer for 10 min. Cells were pelleted by centrifugation at 2, 000 g for 5 min. Next, the anti-IFN-γ-PE/Cy7 antibody was added according to the manufacturer's protocol and incubated for another 40 min in the dark. Subsequently, the cells were washed twice and resuspended in 200 μl FBS-free media for the analysis of T-cell populations with $CD8\alpha^+$ or IFN-γ expression *via* flow cytometry. Similarly, another portion of the single-cell suspension was incubated with anti-mouse CD69-Alexa Fluor 647 and anti-mouse CD49b-Alexa Fluor 488 antibodies for the analysis of the NK-cell population *via* flow cytometry as mentioned previously.

Detection of immune cytokines in tumor

A small section of tumor tissue was lysed with highly efficient lysis buffer supplemented with a proteinase inhibitor cocktail and phosphatase inhibitor (10:1:1). After homogenization, the tissue suspension was centrifuged at 12,000 g for 20 min. The supernatant was reserved for ELISA assays to detect the immune-related factors, including IFN-γ and IL-2, according to the manufacturer's protocol.

Assessment of the biosafety of CD-NPs

To evaluate the biosafety of CD-NPs, the body weights of mice were recorded every other day during the treatment within 2 weeks, and a curve was generated to monitor the weight changes. Moreover, murine blood was acquired before mice were harvested for the hematological and histopathological examination. Briefly, the blood was centrifuged at 4°C for 20 min, and plasma was reserved for blood biochemical analysis, including alanine aminotransferase (ALT) and aspartate aminotransferase (AST) as well as urea (UREA) and creatinine (CREA). In addition, the tumor was fixed and

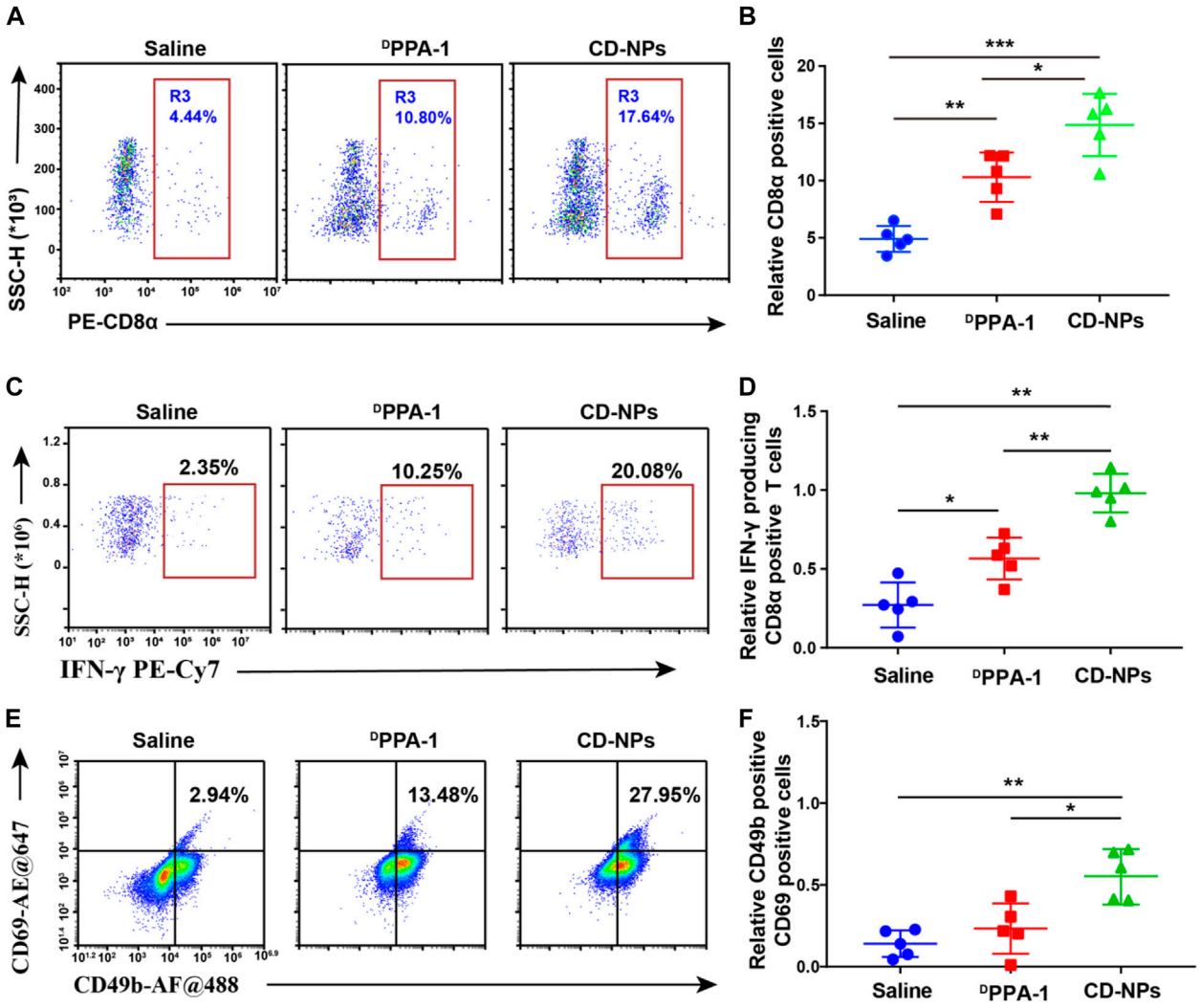

FIGURE 3
Evaluation of antitumor immune responses within tumor tissues. **(A)** Flow cytometry and **(B)** corresponding quantitative analysis of CD8α-positive T cells in the tumor tissue with indicated treatments. **(C)** Flow cytometry and **(D)** corresponding quantitative analysis of IFN-γ-producing CD8α-positive T cells in tumor tissue with indicated treatments. **(E)** Flow cytometry and **(F)** corresponding quantitative analysis of both CD69-positive and CD49-positive NK cells in the tumor tissue with indicated treatments. Data are shown as the mean ± SD; $*p < 0.05$, $**p < 0.01$, $***p < 0.001$.

embedded with paraffin, which was cut for hematoxylin and eosin (H&E) staining to investigate histopathological changes at the end of the therapy.

Data analysis and statistics

All experiments were performed with five parallel samples unless elsewhere indicated, and the result was presented as the mean ± standard deviation (SD). All results were analyzed using GraphPad Prism 7, and Student's t-test was used for statistical analysis ($*p < 0.05$; $**p < 0.01$; and $***p < 0.001$).

Results and discussion

The preparation and characterization of CD-NPs

After modified with hydrophobic octadecanoic acid, the obtained C18-^{D}PPA-1 becomes amphiphilic. When interacted with water molecules, the amphiphilic C18-^{D}PPA-1 tends to expose its hydrophilic segments on the periphery to form an interface with water molecules, while keeps hydrophobic segments inward, consequently assembling into nanostructures. The morphology of the peptide self-assembled nanomedicine was characterized by TEM,

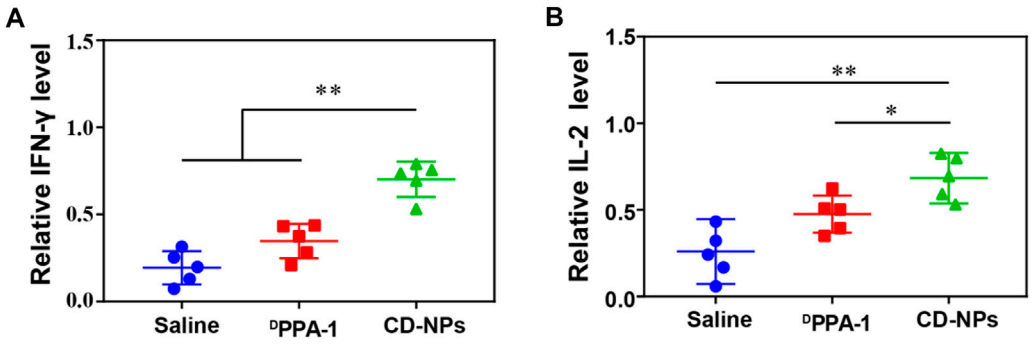

FIGURE 4
Analysis of intratumor immune cytokines. **(A)** Relative levels of IFN-γ and **(B)** IL-2 in the tumor tissue from mice treated with different formulations. Data are shown as the mean ± SD (n = 5); *p < 0.05, **p < 0.01.

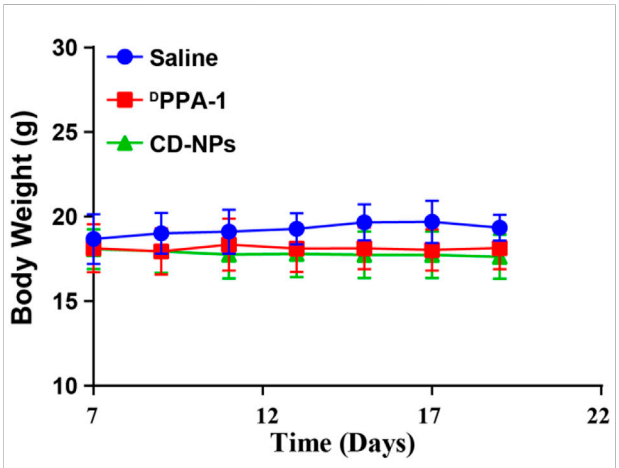

FIGURE 5
Body weight changes in mice treated with different formulations.

and the results showed that the C18-^{D}PPA-1 peptide can form homogenous nanoparticles with a spherical shape (Figure 1A). Also, the hydrodynamic sizes of these nanoparticles were measured with an average size of 35 nm (Figure 1B). The zeta potential of CD-NPs was measured to be c.a. −12.9 ± 1.8 mV. Furthermore, we evaluated the storage stability of CD-NPs. As shown in Figures 1D,E, there are negligible changes in size and zeta potential after incubation in PBS (pH 7.4) for 5 days, implying the good storage stability of CD-NPs.

Evaluation of the antitumor efficacy of CD-NPs *in vivo*

It is well known that the blood clearance time is critical for drugs to work *in vivo*. Before evaluating the antitumor effect, we study the pharmacokinetics of prepared CD-NPs. The CY5 fluorescence dye was used to covalently label the ^{D}PPA-1 peptide and CD-NPs. After being intravenously injected into mice, the CY5-labeled ^{D}PPA-1 was quickly cleared (Figure 2A). Significantly, the prepared CD-NPs prolonged the circulation time with a half-life time of 1.45 h (CY5-CD-NPs) vs. 0.44 h (CY5-^{D}PPA-1), which facilitates the antitumor response *in vivo* (Figure 2B). To visually monitor the antitumor effect, the bioluminescence images of mice were recorded during the whole trials. As shown in Figure 2C, the tumors in each group had similar size before the treatment and revealed distinct growing rates during the treatment. In addition, the analysis of bioluminescence signals demonstrated that the luciferase signal in the ^{D}PPA-1 group was 1.3 times higher than that in the CD-NP group, indicating that the ^{D}PPA-1 has the antitumor effect but not as good as the CD-NPs, which only had about half of the luciferase signal of the saline group with statistical significance in the tumor inhibition (Figure 2D). According to the tumor growth curves, we found that the tumor volumes in the group treated with saline reached about 1000 mm^3 at the end of therapy, while the tumor volumes in the group treated with ^{D}PPA-1 were about 560 mm^3, showing a mild tumor inhibition rate. In contrast, the tumor volumes of the group treated with CD-NPs were only about 350 mm^3 (Figure 2E), which further demonstrated that the CD-NPs indeed had better antitumor efficacy. Similar inhibition tendency was observed in the tumor weight, as the results showing the average tumor weight in the CD-NP groups was only 1/2 and 3/5 of that in the saline group and ^{D}PPA-1 group, respectively (Figure 2F).

Evaluation of the antitumor immune response of CD-NPs *in vivo*

Given that the antitumor effect of nanomedicine is closely associated with the tumor-infiltrating immune cells in the tumor tissues, we further analyzed the tumor-infiltrating immune cell populations with flow cytometry to elucidate the mechanism of the higher antitumor efficacy of CD-NPs than the ^{D}PPA1 peptide

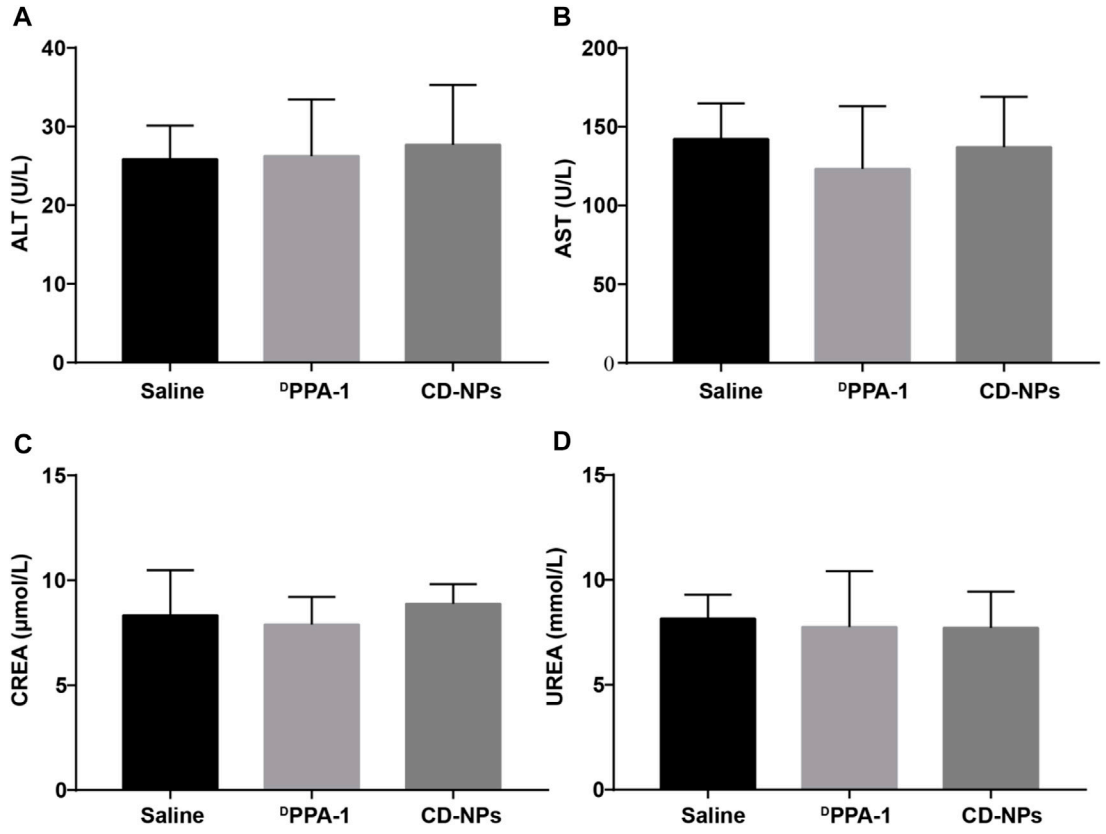

FIGURE 6
Blood biochemical level analysis of mice after treatments. Levels of **(A)** alanine aminotransferase (ALT) and **(B)** aspartate aminotransferase (AST) as well as **(C)** serum creatinine (CREA) and **(D)** urea (UREA) in blood from mice treated with different formulations. Data are shown as the mean ± SD (n = 3).

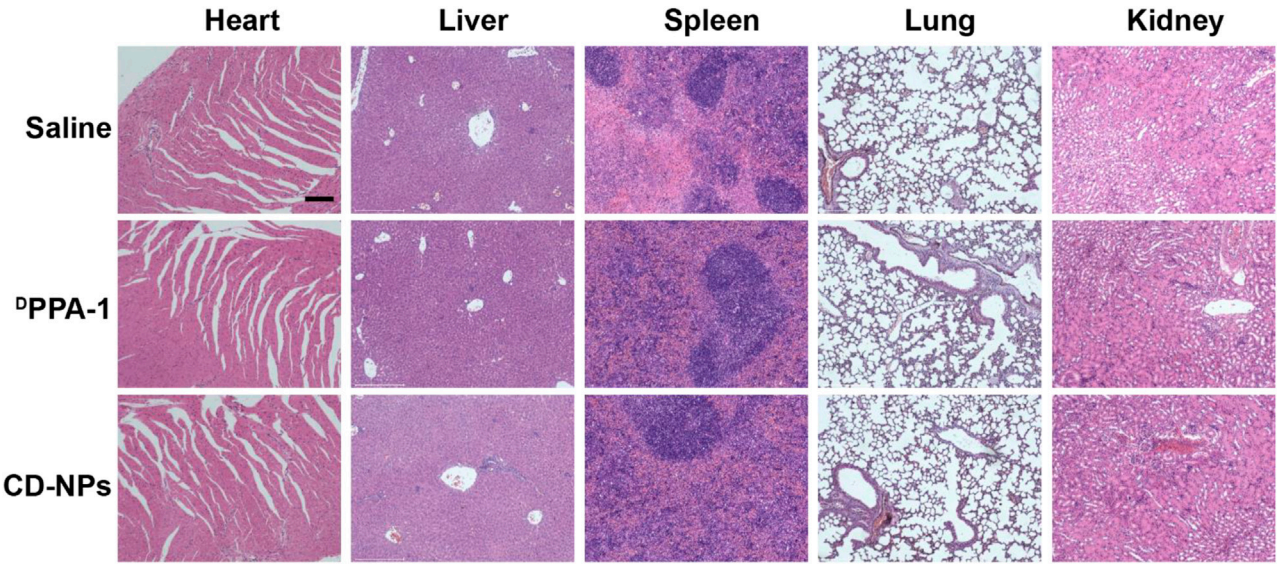

FIGURE 7
Representative images of H&E staining of hearts, livers, spleens, lungs, and kidneys of mice treated with different formulations. Scale bars, 200 μm.

observed *in vivo*. As shown in the results, CD8α-positive ($CD8\alpha^+$) T cells and IFN-γ-producing $CD8\alpha^+$ T-cell populations were obviously elevated to a level of 17.64% and 20.08%, respectively, which is approximately 4 times and 1.5 times of those in saline and ^{D}PPA-1 groups (Figures 3A–D). The enhanced infiltration of tumor immune cells could benefit from the unique characteristics of nanomedicine that they can extend the half-life and the retention in the tumor tissues. In addition, we observed a higher population of NK cells ($CD69^+$ $CD49b^+$) in the CD-NP group, which is 2.6 times and 1.8 times of that in the groups treated with saline and ^{D}PPA1, respectively (Figures 3E,F). Taken together, the peptide self-assembled nanomedicine could activate the immune response and increase the effector T cells and NK cells in the tumor microenvironment.

We further detected the intratumor immune-related cytokines to reveal the antitumor immune response activation of nanomedicine. The ^{D}PPA-1 was found to mildly increase the levels of IFN-γ and IL-2, while CD-NPs caused significant elevation in these cytokines (Figures 4A,B). This result demonstrated that the peptide-based nanomedicine can block the PD-1/PD-L1 interaction to enhance the antitumor effect by activating the immune response and increasing the immune cytokines in the tumor microenvironment.

Evaluation of the biosafety of CD-NPs *in vivo*

To assess the biosafety of CD-NPs *in vivo*, the body weights of mice in each group were recorded during the treatment, and no obvious changes were found in any groups during the treatment (Figure 5), indicating that CD-NPs barely impact the normal growth of mice.

In addition, murine blood was collected for the hematological and histopathological examination for monitoring the liver and kidney function. We found that there were no obvious changes in ALT and AST as well as the CREA and UREA levels (Figure 6), implying that the liver and kidney function was not impacted by CD-NPs. This result demonstrates that the CD-NPs do not cause liver or kidney toxicity.

At the end of therapy, mice were sacrificed, and tissues including the heart, liver, spleen, lung, and kidney were harvested for hematoxylin and eosin (H&E) staining to investigate histopathological changes. No obvious changes in the tissues were observed (Figure 7), indicating that no harm to the major tissues was caused by CD-NPs during the treatment. Taken together, CD-NPs have good biocompatibility with minimal toxicity *in vivo*.

Conclusion

In summary, this work constructed an amphiphilic peptide through a practical chemical modification based on ^{D}PPA-1 peptide. The amphiphilic peptide can self-assemble into a spherical nanomicelle (CD-NPs). The *in vivo* antitumor study showed that the prepared CD-NPs can effectively inhibit the growth of 4T1 tumors. Furthermore, immuno-analysis revealed that CD-NPs can evoke the host immunity through improving the infiltration of T cells and NK cells and elevating the level of antitumor immune cytokines in the tumor tissue. Moreover, good biocompatibility of CD-NPs was further confirmed through body weight monitoring, biochemical analysis, and histopathological examination. Taken together, this work developed practical peptide-based ICIs for tumor immunotherapy. Owing to the superiority of controllable cost, good storage stability, and significant antitumor activity, the prepared CD-NPs host great potentials for immunotherapy. However, the majority of tumor patients do not benefit from ICI-based therapy because of the "cold" tumor microenvironment and other tumor-associated factors. The development of a synergistic strategy to overcome the drawbacks of ICI-based therapy is of significance in the clinic in the future.

Data availability statement

The original contributions presented in the study are included in the article/Supplementary Material; further inquiries can be directed to the corresponding authors.

Ethics statement

The animal study was reviewed and approved by the Zhengzhou University Institutional Animal Care and Use Committee.

Author contributions

TH, YQ, and HG conceived and designed the experiments. XS, XM, MC, and YL performed the experiments and analyzed the data. TH, YQ, and SD wrote the original draft. YQ and HG supervised the project and revised the original draft. HG conceptualized and supervised the project. All authors have read and agreed to the published version of the manuscript.

Funding

This work was supported by the National Natural Science of Foundation of China (32000998), Natural Science

Foundation of Chinese Postdoctoral (2019TQ0285 and 2019M662513), Science and Technology Joint Project of Henan Province (LHGJ20210210), and Science and Technology Development Project of Henan Province (222102310525 and 212102310138).

Acknowledgments

The authors would like to acknowledge the use of resources at the Center of Advanced Analysis and Gene Sequencing, Zhengzhou University, and the National Center for Nanoscience and Technology.

Conflict of interest

The authors declare that the research was conducted in the absence of any commercial or financial relationships that could be construed as a potential conflict of interest.

Publisher's note

All claims expressed in this article are solely those of the authors and do not necessarily represent those of their affiliated organizations, or those of the publisher, the editors, and the reviewers. Any product that may be evaluated in this article, or claim that may be made by its manufacturer, is not guaranteed or endorsed by the publisher.

References

Acurcio, R. C., Scomparin, A., Conniot, J., Salvador, J. A. R., Satchi-Fainaro, R., Florindo, H. F., et al. (2018). Structure-function analysis of immune checkpoint receptors to guide emerging anticancer immunotherapy. *J. Med. Chem.* 61, 10957–10975. doi:10.1021/acs.jmedchem.8b00541

Blank, C., and Mackensen, A. (2007). Contribution of the PD-L1/PD-1 pathway to T-cell exhaustion: An update on implications for chronic infections and tumor evasion. *Cancer Immunol. Immunother.* 56, 739–745. doi:10.1007/s00262-006-0272-1

Chang, H. N., Liu, B. Y., Qi, Y. K., Zhou, Y., Chen, Y. P., Pan, K. M., et al. (2015). Blocking of the PD-1/PD-L1 interaction by a D-peptide antagonist for cancer immunotherapy. *Angew. Chem. Int. Ed.* 54, 11760–11764. doi:10.1002/anie.201506225

Chen, D. S., and Mellman, I. (2013). Oncology meets immunology: The cancer-immunity cycle. *Immunity* 39, 1–10. doi:10.1016/j.immuni.2013.07.012

Cheng, K., Ding, Y., Zhao, Y., Ye, S., Zhao, X., Zhang, Y., et al. (2018). Sequentially responsive therapeutic peptide assembling nanoparticles for dual-targeted cancer immunotherapy. *Nano Lett.* 18, 3250–3258. doi:10.1021/acs.nanolett.8b01071

Cui, H. G., Webber, M. J., and Stupp, S. I. (2010). Self-assembly of peptide amphiphiles: From molecules to nanostructures to biomaterials. *Biopolymers* 94, 1–18. doi:10.1002/bip.21328

Darvin, P., Toor, S. M., Nair, V. S., and Elkord, E. (2018). Immune checkpoint inhibitors: Recent progress and potential biomarkers. *Exp. Mol. Med.* 50, 1–11. doi:10.1038/s12276-018-0191-1

Delfi, M., Sartorius, R., Ashrafizadeh, M., Sharifi, E., Zhang, Y. P., De Berardinis, P., et al. (2021). Self-assembled peptide and protein nanostructures for anti-cancer therapy: Targeted delivery, stimuli-responsive devices and immunotherapy. *Nano Today* 38, 101119. doi:10.1016/j.nantod.2021.101119

Dempke, W. C. M., Fenchel, K., Uciechowski, P., and Dale, S. P. (2017). Second- and third-generation drugs for immuno-oncology treatment-The more the better? *Eur. J. Cancer* 74, 55–72. doi:10.1016/j.ejca.2017.01.001

Du, C., Qi, Y., Zhang, Y., Wang, Y., Zhao, X., Min, H., et al. (2018). Epidermal growth factor receptor-targeting peptide nanoparticles simultaneously deliver gemcitabine and olaparib to treat pancreatic cancer with breast cancer 2 (BRCA2) mutation. *Acs Nano* 12, 10785–10796. doi:10.1021/acsnano.8b01573

Eskandari, S., Guerin, T., Toth, I., and Stephenson, R. J. (2017). Recent advances in self-assembled peptides: Implications for targeted drug delivery and vaccine engineering. *Adv. Drug Deliv. Rev.* 110, 169–187. doi:10.1016/j.addr.2016.06.013

Gautam, A., Kapoor, P., Chaudhary, K., Kumar, R., Raghava, G. P. S., and Open Source Drug Discovery, C. (2014). Tumor homing peptides as molecular probes for cancer therapeutics, diagnostics and theranostics. *Curr. Med. Chem.* 21, 2367–2391. doi:10.2174/0929867321666140217122100

Gong, N. Q., Sheppard, N. C., Billingsley, M. M., June, C. H., and Mitchell, M. J. (2021). Nanomaterials for T-cell cancer immunotherapy. *Nat. Nanotechnol.* 16, 25–36. doi:10.1038/s41565-020-00822-y

Hu, C., He, X. Q., Chen, Y. X., Yang, X. T., Qin, L., Lei, T., et al. (2021). Metformin mediated PD-L1 downregulation in combination with photodynamic-immunotherapy for treatment of breast cancer. *Adv. Funct. Mat.* 31, 2007149. doi:10.1002/adfm.202007149

Li, Z., Ding, Y., Liu, J., Wang, J., Mo, F., Wang, Y., et al. (2022). Depletion of tumor associated macrophages enhances local and systemic platelet-mediated anti-PD-1 delivery for post-surgery tumor recurrence treatment. *Nat. Commun.* 13, 1845. doi:10.1038/s41467-022-29388-0

Li, Z., Wang, Y., Shen, Y., Qian, C., Oupicky, D., and Sun, M. (2020). Targeting pulmonary tumor microenvironment with CXCR4-inhibiting nanocomplex to enhance anti–PD-L1 immunotherapy. *Sci. Adv.* 6, eaaz9240. doi:10.1126/sciadv.aaz9240

Mahoney, K. M., Freeman, G. J., and McDermott, D. F. (2015). The next immune-checkpoint inhibitors: PD-1/PD-L1 blockade in melanoma. *Clin. Ther.* 37, 764–782. doi:10.1016/j.clinthera.2015.02.018

Marin-Acevedo, J. A., Dholaria, B., Soyano, A. E., Knutson, K. L., Chumsri, S., and Lou, Y. Y. (2018). Next generation of immune checkpoint therapy in cancer: New developments and challenges. *J. Hematol. Oncol.* 11, 39. doi:10.1186/s13045-018-0582-8

Meng, X. J., Huang, Z. Q., Teng, F. F., Xing, L. G., and Yu, J. M. (2015). Predictive biomarkers in PD-1/PD-L1 checkpoint blockade immunotherapy. *Cancer Treat. Rev.* 41, 868–876. doi:10.1016/j.ctrv.2015.11.001

Rezvani, K., Rouce, R., Liu, E. L., and Shpall, E. (2017). Engineering natural killer cells for cancer immunotherapy. *Mol. Ther.* 25, 1769–1781. doi:10.1016/j.ymthe.2017.06.012

Robert, C. (2020). A decade of immune-checkpoint inhibitors in cancer therapy. *Nat. Commun.* 11, 3801. doi:10.1038/s41467-020-17670-y

Singh, S., Hassan, D., Aldawsari, H. M., Molugulu, N., Shukla, R., and Kesharwani, P. (2020). Immune checkpoint inhibitors: A promising anticancer therapy. *Drug Discov. Today* 25, 223–229. doi:10.1016/j.drudis.2019.11.003

Sun, Z. L., Zhang, Y., Cao, D., Wang, X. F., Yan, X. B., Li, H., et al. (2018). PD-1/PD-L1 pathway and angiogenesis dual recognizable nanoparticles for enhancing chemotherapy of malignant cancer. *Drug Deliv.* 25, 1746–1755. doi:10.1080/10717544.2018.1509907

Taleb, M., Atabakhshi-Kashi, M., Wang, Y., Rezavani Alanagh, H., Farhadi Sabet, Z., Li, F., et al. (2021). Bifunctional therapeutic peptide assembled nanoparticles exerting improved activities of tumor vessel normalization and immune checkpoint inhibition. *Adv. Healthc. Mat.* 10, 2100051. doi:10.1002/adhm.202100051

Yu, L., Dou, S. B., Ma, J. H., Gong, Q., Zhang, M. G., Zhang, X. Q., et al. (2021). An antimicrobial peptide-loaded chitosan/polyethylene oxide nanofibrous membrane fabricated by electrospinning technology. *Front. Mat.* 8. doi:10.3389/fmats.2021.650223

Zhao, Y., Ji, T., Wang, H., Li, S., Zhao, Y., and Nie, G. (2014). Self-assembled peptide nanoparticles as tumor microenvironment activatable probes for tumor targeting and imaging. *J. Control. Release* 177, 11–19. doi:10.1016/j.jconrel.2013.12.037